academicJournals

Vol. 7(50), pp. 5613-5624, 18 December, 2013
DOI: 10.5897/AJMR2013.5791
ISSN 1996-0808 ©2013 Academic Journals
http://www.academicjournals.org/AJMR

African Journal of Microbiology Research

Full Length Research Paper

Quantitative PCR analysis of diesel degrading genes of *Acinetobacter calcoaceticus* isolates

Johnson Lin*, Vikas Sharma and RakshaToolsi

School of Life Sciences, University of KwaZulu-Natal (Westville), Private Bag X 54001, Durban, Republic of South Africa.

Accepted 18 November, 2013

Acinetobacter **strains LT_1 and V_2 were grown in Bushnell-Haas medium with 1% diesel and their expression levels of eight diesel-degrading genes were evaluated by quantitative polymerase chain reaction (PCR). LT_1 and V_2 isolates achieved 86.2 and 89.7% degradation respectively, after 60 days with no significant differences in expression, in comparison with 16S rRNA, *rub*B and *lip*B. LT_1 showed higher expression levels of *rub*A, *alk*M, *alk*R and *xcp*R genes during the initial stages of incubation corresponding to higher level of degradation rate. Amplification of *alk*M, *alk*R and *xcp*R genes of V_2 indicated more than one enzyme system involved in the process. Low *lip*B and *lip*A expression in LT_1 and no *lip*A expression in V_2 suggested the absence of lipases in degradation; however, *est*B gene was predominantly expressed in V_2. Thus, isolates LT_1 and V_2 possessed comparable efficiency in degrading diesel; however, more complex systems have been employed by V_2i n degradation process.**

Key words: qPCR, diesel degradation, *Acinetobacter calcoaceticus,* bioemulsifier, gene expression.

INTRODUCTION

A wide array of studies has dealt with biodegradation and bioremediation of petroleum hydrocarbon unraveling the intricacies of degradation and generating a wealth of bacterial, genetic, biochemical, and physiological knowledge (van Beilen and Funhoff, 2007; Rojo, 2009). Characterization of bacterial communities, isolation of prospective degraders, monitoring their response to pollutants, and identifying functional genes and enzymes involved in biodegradation processes have been subject to extensive research (Wentzel et al., 2007; Rojo, 2010). Over the years, a multitude of bacterial species capable of degrading hydrocarbon, have been readily isolated from hydrocarbon-contaminated and non-contaminated sites. *Acinetobacter* sp. are one of the representative genera capable of utilizing *n*-alkanes (Tani et al., 2002; Van Hamme et al., 2003; Singh and Lin, 2008; Lee et al., 2012; Mara et al., 2012).

The pathways of alkane degradation and the enzymes involved in it have been reviewed extensively (Coon, 2005; van Beilen and Funhoff, 2007; Wentzel et al., 2007; Rojo 2010). In majority of the cases, aerobic degradation of n-alkanes starts either by the terminal (van Beilen and Funhoff, 2007; Wentzel et al., 2007; Rojo 2010) or sub-terminal oxidation pathway (Kotani et al., 2006). In this pathway, conversion of methyl group which leaves a primary alcohol, is further oxidized to the corresponding aldehyde, fatty acid and finally processed by β–oxidation pathway to generate acetyl-CoA (Wentzel et al., 2007; Rojo 2010). In some microorganisms, both terminal and sub-terminal oxidation pathway coexists (Watkinson and Morgan, 1990).

In *Acinetobacter calcoaceticus*, alkane hydroxylases

*Corresponding author. E-mail: linj@ukzn.ac.za. Tel: +27-31-2607407. Fax: +27-31-2607809.

(encoded *alk*M) require two soluble electron transfer proteins named rubredoxin (*rub*A) and rubredoxinreductase (*rub*B) for *n*-alkane degradation and are obligatory for its function (Tani et al., 2001). The *alk*M gene expression is regulated by the alkane hydroxylase regulator (*alk*R) (Ratajczak et al., 1998). The participation of *xcpR* gene in alkane degradation was proposed in *A. calcoaceticus* ADP1 after the insertional inactivation of *xcpR* impeded the secretion of lipase and esterase that lead to the lack of growth on dodecane and slower growth on hexadecane (Parche et al., 1997). In *A. calcoaceticus* ADP1, the *est*B gene encodes a functional esterase and is localized in an operon with genes *rub*A, *rub*B and *oxy*R (Geißdörfer et al. 1999). The esterase activity has been reported to be involved in the sub-terminal oxidation pathway (Kotani et al., 2007). The involvement of these enzymes in the degradation of hydrocarbons has been proposed, however their exact function is unknown.

Genomes of many *Acinetobacter* strains have been sequenced recently, including those of *Acinetobacter* sp. DR1 (Jung et al., 2010), *Acinetobacter oleivoran s*sp. DR1(T) (Kang et al., 2011), *Acinetobacter venetianus*RAG-1T (Fondi et al., 2012) and *Acinetobacter venetianus*VE-C3 (Fondi et al., 2013). Although, momentous gains have been made in understanding the processes in hydrocarbon degradation, the minutiae of individual systems as well as the diversity of systems have yet to be fully articulated (Van Hamme et al., 2003). Therefore, this study investigated the proficiency of *A. calcoaceticus* isolates in the degradation of diesel and implementing the levels of mRNA expression of diesel degrading genes using quantitative polymerase chain reaction.

MATERIALS AND METHODS

Selection and identification of diesel degrading bacterial isolates

A. calcoaceticus isolates $LT_1$and V_2, were obtained from departmental stock cultures. LT_1 (accession number JN036553) were originally isolated from diesel-contaminated soil (Singh and Lin, 2008) while V_2 (accession number JN036552) was isolated from used engine oil-contaminated soil (Mandri and Lin, 2007) previously from the same laboratory Isolates were streaked on nutrient agar and incubated at 30°C for 24 h to attain pure cultures.

Growth of bacterial isolates on diesel as sole carbon and energy source

To access their ability to degrade diesel, isolates were grown on Bushnell-Haas (BH) minimal medium with diesel as sole carbon source (Singh and Lin, 2008). Isolates were grown in separate 100 ml Erlenmeyer flasks with a total volume of 25 ml of liquid BH medium supplemented with 1% (vol/vol) sterilized diesel using 0.22 µm membrane filters (Whatman) as a carbon and energy source. The isolates were grown overnight at 30°C in Luria broth, washed thrice with normal saline and 1% of the washed cells were inoculated in each BH medium (standardized using BH medium to OD_{600} of 1.0 after centrifugation). The BH medium flasks were incubated aerobically at 30°C in a rotary shaker (160 rpm) for variable time period. An abiotic control flask, with 1% (vol/vol) diesel and devoid of bacterial inoculum, was incubated under the same conditions to ascertain abiotic loss. Bacterial growth was monitored by optical density at 600 nm (OD_{600}) at 5, 10, 15, 20, 30, 40, 50 and 60 days of incubation. The experiments were repeated in triplicate.

Carbon source utilisation patterns were determined by gravimetric analysis (Marquez-Rocha et al., 2001). The remaining diesel in each sample was extracted using the separating funnel with 10 ml dichloromethane three times. The dichloromethane extract was funneled through filter paper containing 5 g anhydrous sodium sulfate (Na_2SO_4) for the removal of cellular debris and absorption of moisture. The extract was collected in the pre-weighed glass tubes and was left overnight in a fume cupboard to facilitate evaporation of dichloromethane. The combined mass of the pre-weighed tube and diesel was recorded. The mass of the tube was subtracted to determine the mass of the diesel remaining. The mass of the diesel remaining was subtracted from the mass of diesel in the control sample and multiplied by 100 to determine the percentage of diesel remaining. Student t-test (Microsoft Excel 2010) was used to evaluate the differences of diesel degradation between LT_1 and V_2. Probability (significant level) was set at 0.05.

RNA extraction and cDNA validation

The BH medium containing isolates was centrifuged at 4000 x*g* for 20 min resulting in a pellet and a cell-free supernatant. Pellet was re-suspended in phosphate-buffered saline (PBS), pH 7.6, and subjected to further centrifugation at 4000 x*g* for 20 min. Total RNA was extracted from each pellet using Aurum ^{TM} Total RNA Mini Kit (BIO-RAD) according to manufacturer's instructions with following modifications :500 µl of lysozyme was added instead of 100 µl of 1000 µg/ml stock dissolved in TE (10 mMTris, 1mM EDTA, pH 7.5) to the bacterial suspension and incubated at room temperature for 30 min. Total RNA purity and yield was determined spectrophotometrically using Nanodrop ND-1000 (BIO-RAD). Purified RNA (1 µg) was used to prepare cDNA by using a first Strand iScript^{TM} cDNA Synthesis Kit (BIO-RAD). The reverse transcriptase PCR was performed (GeneAmp® PCR System 9700, Applied Biosystems) according to manufacturer's instructions. Purified RNA and cDNAwas also assessed electrophoretically by ethidium bromide staining on 2% (wt/vol) agarose in 1 X TAE running buffer at 80V. The $OD_{260/280}$ ratio obtained ranged from 1.30 to 2.27. Samples LT_1 - day 5, with ratio of 1.30, indicated poor RNA quality that resulted in no 16S rRNAPCR product detected. LT_1 - day 5 sample was omitted from the real time PCR study.The PCR product of 16S rRNA gene using 63F and 1387R primers (Marchesi et al., 1998) was obtained. DNA concentrations of 16S rRNA PCR products were measured spectrophotometrically using a NanoDrop ND-1000 spectrophotometer and concentrated stock solutions of specific 16S rRNA gene fragments were prepared. These were serially diluted to generate a set of calibration pure standards with known concentrations of target DNA.The cDNA obtained was stored at -20°C.

Real-time PCR data analysis and quantification of gene expression

The nucleotide sequences of the genes of interest were acquired from the National Center for Biotechnology Information (NCBI) nucleotide sequence databases with the following accession numbers: AF047691 (*lip*A and *lip*B), AJ233398 (*alk*M and *alk*R), EF524340 (16S rRNA), Y09102 (*xcp*R) and Z46863 (*rub*A, *rub*B,

Table 1. Primers sequences for real-time PCR amplification of target genes.

Primer	Sequence	Product size (bp)
16S rRNA		
Forward	5'-GTAGCGGGTCTGAGAGGATG-3'	169
Reverse	5'-GCCTCCTCCTCGCTTAAAGT-3'	
*rub*A (rubredoxin)		
Forward	5'-GATTTATGATGAAGCCGAAGG-3'	91
Reverse	5'-GTCAGGGCAAGTCCAGTCAT-3'	
*rub*B (rubredoxin reductase)		
Forward	5'-GCCCACTGGGTCGTCTATTA-3'	222
Reverse	5'-CGTGTTTTGCCAGATCAATG-3'	
*alk*M (alkane hydroxylase)		
Forward	5'-AAAGATGCGCGTAATCCAAC-3'	189
Reverse	5'-ATTAATGGCACCCATCGAAA-3'	
*alk*R (alkane hydroxylase regulator)		
Forward	5'-TGTAGCATGATGCGCTTTTC- 3'	161
Reverse	5'-CACAAGGTGAATGGGCTTTT- 3'	
*est*B (esterase)		
Forward	5'-ATCCAAAATTCGCCACAAAG-3'	150
Reverse	5'-TTTTTAATCCGCATCGCTTC-3'	
*Lip*A (lipase)		
Forward	5'-CTTCCGTTTCAACGATTGGT- 3'	189
Reverse	5'-TATACGCTGCACCGACAGAG- 3'	
*lip*B (lipase)		
Forward	5'-CCAACCCTAGCAGCATCATT- 3'	153
Reverse	5'-TGCAACAAGCTCTGCTTCAG- 3'	
*xcp*R (a subunit of the general secretion pathway for exoproteins)		
Forward	5'-AGGGTTAATGGCGGAAGACT-3'	192
Reverse	5'-CCAATCCCTTCGAGCTGATA-3'	

and *est*B). Primers for real-time PCR were designed with the aid of primer design software Primer3 (Kubista et al., 2006) and were synthesized by Inqaba Biotech. The real-time PCR primer sequences are presented in Table 1.

PCR amplifications of *alk*M, *alk*R, *rub*A, *rub*B, *est*B, *lip*A, *lip*B, *xcp*R and 16S rRNA genes were performed using LightCycler® Instrument Version 3.5real-time PCR system (RocheDiagnostics). LightCycler® reactions were performed in 20 µl glass capillary tubes using LightCycler® FaststartDNA Master SYBR Green I kit (Roche Diagnostics) according to the manufacturer's instructions. The evaluating parameters selected for data analysis were fluorescence (d[F1]/dT), melting temperature (T_m) and crossing point (C_p) (Pfaffl et al., 2002; Rasmussen, 2001). Conditions of real-time PCR for the respective target genes under the optimized conditions are presented in Table 2. Specificity of real-time PCR primers was determined using LightCycler Software®, Version 3.5 (Roche Diagnostics). Due to the multiple products in some samples, the cDNA of $LT_1$was selected as the calibrator for 16S rRNA, *alk*M, *alk*R, *rub*A, *lip*A, *lip*B and *xcp*R genes and that of $V_2$for *est*B gene. Each amplification product for the target genes demonstrated a specific and characteristic melting curve (supplementary Figure 1S). Specificity of real-time PCR products were documented by agarose gel electrophoresis and resulted in a single product of anticipated length. No PCR amplification product was observed for gene *rub*B, despite rigorous optimization strategies and redesigning of primers.

Equal aliquots of cDNA obtained were standardized to 1000 ng/µl.

To generate a standard curve, the serially diluted cDNA standard (1,000 to 0.001 ng) was quantified in each real-time PCR runin duplicates. The efficiency of each standard curve was determined using the equation: Efficiency (E) = $10^{-1/slope}$ - 1 (Rasmussen, 2001). Descriptive statistics (minimal (Min) and maximal (Max) mean values, standard deviation (SD), and coefficient of variance (CV %), of the derived C_p values were computed for each investigated gene to determine intra-sample variation.

Gene expression was quantified using the Pfaffl model which combines gene quantification and normalizationand was calculated with the aid of Microsoft Excel® based application, Relative Expression Software Tool - XL (REST-XL©) - Version 2 (Pfaffl et al., 2002). The C_p values of both, control and the samples of interest were normalized based on the PCR product of 16S rRNA gene in each sample. The copy number of each gene was calculated based on the 16S rRNA standard curve.

RESULTS AND DISCUSSION

Growth of bacterial isolates on diesel and their carbon utilization pattern

The growth behavioral patterns of the bacterial isolates on diesel were monitored over a period of 60 days and determined by optical density (OD_{600}). The results obtained

Table 2. Composition of reaction Mastermix and amplification parameters for LightCycler®real-time PCR assays.

Target gene	Primer conc. (pmol/µl)	Reaction components (µl)*					Amplification parameter
		DEPC H_2O	Forward primer	Reverse primer	$MgCl_2$ (25 mM)	SYBR green	
16S rRNA	1.25	5.8	0.5	0.5	1.2	1.0	30 cycles of 5 s at 95°C (Denaturing), 10 s at 62°C (Annealing), 5 s at 72°C (Polymerizing)
*alk*M	10.0	6.0	0.5	0.5	1.0	1.0	50 cycles of 5 s at 95°C, 15 s at 62°C, 5 s at 72°C
*alk*R	5.00	6.2	0.5	0.5	0.8	1.0	55 cycles of 5 s at 95°C, 8 s at 62°C, 5 s at 72°C
*rub*A	5.00	5.8	0.5	0.5	1.2	1.0	40 cycles of 5 s at 95°C, 15 s at 62°C, 5 s at 72°C
*lip*A	10.0	5.8	0.5	0.5	1.2	1.0	55 cycles of 5 s at 95°C, 10 s at 62°C, 5 s at 72°C
*lip*B	10.0	5.8	0.5	0.5	1.2	1.0	55 cycles of 5 s at 95°C, 10 s at 62°C, 5 s at 72°C
*xcp*R	10.0	5.8	0.5	0.5	1.2	1.0	55 cycles of 5 s at 95°C, 10 s at 62°C, 5 s at 72°C
*est*B	10.0	5.8	0.5	0.5	1.2	1.0	55 cycles of 5 s at 95°C, 15 s at 60°C, 5 s at 72°C

*Final reaction volume of 9 µl.

obtained are presented in Figure 1. After 60 days of incubation, a 9.40% mass reduction in the diesel of the abiotic control flask was detected (data not shown). Both isolates displayed comparable proficiency in the overall utilization of diesel as a sole carbon and energy source. Rapid degradation of alkanes occurred during the first 5 days of incubation with attributes to the exponential growth phase of the bacterial cells. The $OD_{60\ 0}$increased progressively up to 15 days, and remained relatively constant until the end of the culture time. Both isolates LT_1 and V_2 showed diesel degrading capability. LT_1 and V_2 achieved 58.6 and 48.3% degradation after 5 days of incubation and 86.2and 89.7% degradation after 60 days of incubation, respectively (Figure 1). During the initial days of incubation, V_2 degraded less diesel as compared to LT_1. However, after a rapid increase in diesel degradation at day 15, V_2 emerged as the most proficient diesel degrader by the end of the incubation period (Figure 1), though the diesel degradation ability between these two strains did not differ significantly (p=0.506) at the end of the experiment.

The presence of an opaque substance was observed in the hydrocarbon and hydrocarbon - culture medium fraction of V_2 samples throughout the incubation process. After 10 days of incubation, however, the diesel of the V_2 samples no longer appeared as a confluent layer over the culture medium phase, but rather as minuscule droplets. This occurrence was not observed for LT_1 samples for the duration of the culture time.

Optimizing the components of the real-time PCR master mix

LightCycler analyses of *alk*M, *alk*R, *rub*A, *rub*B, *xcp*R, *est*B, *lip*A, *lip*B and16S rRNA were performed and optimized. Melting temperature (T_m) of target gene amplification products ranged from 79.3°C for *alk*R to 91.2°C for 16 rRNA (Figure 1S). A high degree of efficiency ranging from 1.76 to 2.24 was achieved indicating a stable and reliable assay. All generated standard curves illustrated high linearity with r^2 values of 1.00 over three orders of magnitude. An expression profile of *lip*A could not be created for LT_1, and V_2 samples due to very low expression levels of *lip*A and therefore, E_{lipA} could not be deter-

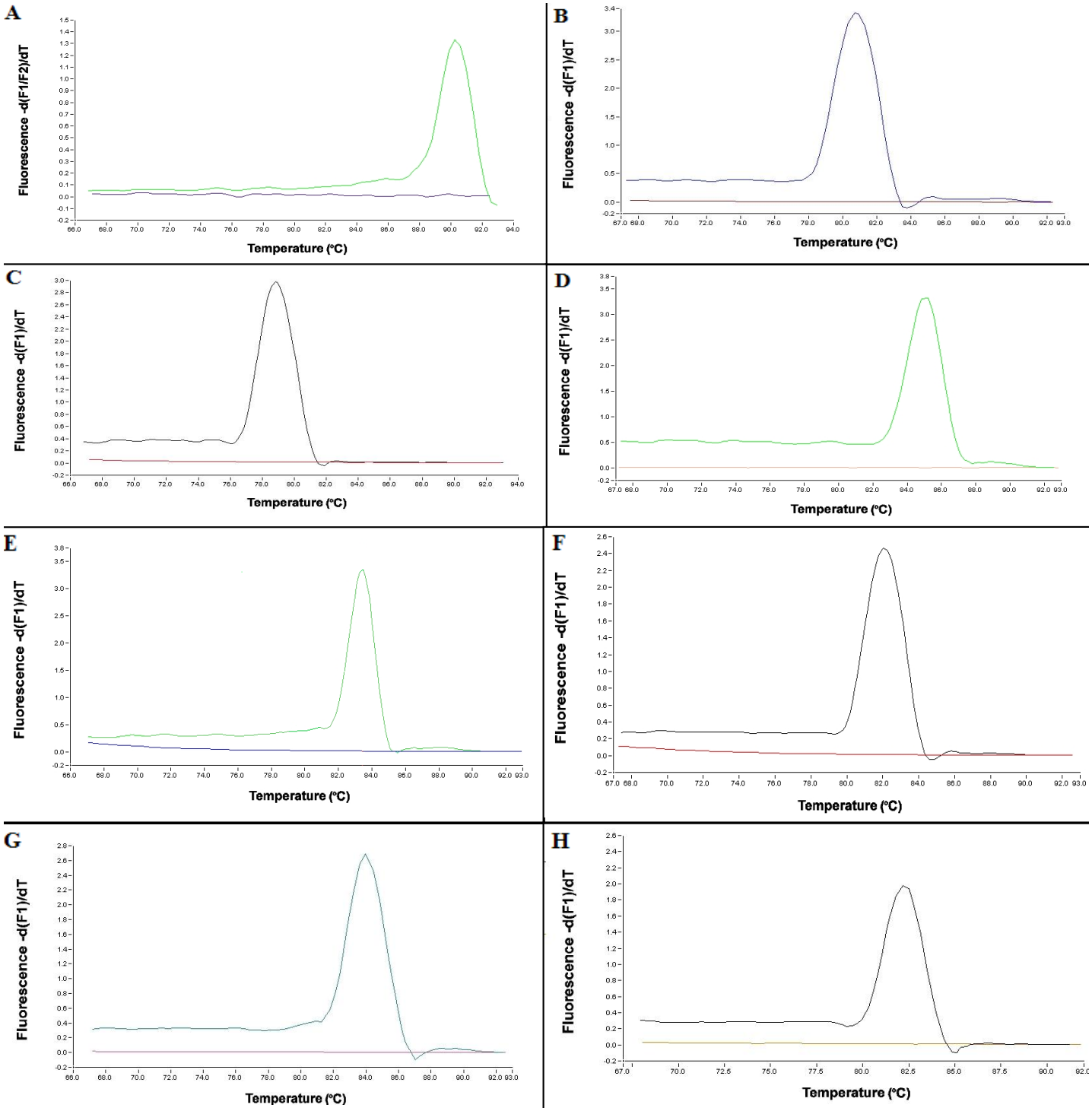

Figure 1S. Specificity of LightCycler® PCR. Amplification of target genes (A) 16S rRNA, (B) *alk*M, (C) *alk*R, (D) *rub*A, (E) *lip*A, (F) *lip*B, (G) *xcp*R, and (H) *est*B, as determined by melting curve analysis. Melting peaks were determined by plotting the continuous negative derivative of fluorescence emitted by each sample as PCR products were melted. The cDNA template control sample for each reaction does not show fluorescence, confirming the absence of primer-dimers.

mined. E_{alkR} yielded an efficiency of 2.24, exceeding the maximum permissible efficiency of 2 (E = 100%), indicating an inappropriately optimized assay and/or poor specificity of primer pairs.

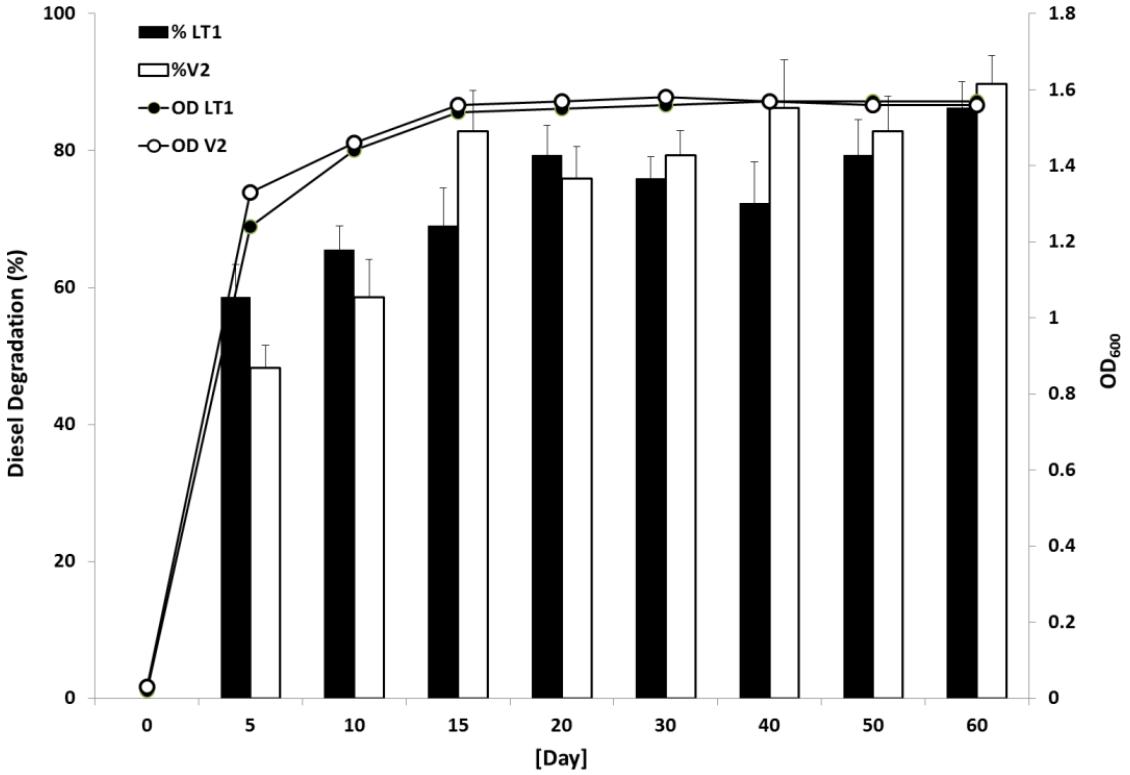

Figure 1. Diesel degradation (%) and growth (OD_{600}) patterns of *A. calcoaceticus* isolates.

The 16S rRNA gene was stably expressed in LT_1 samples throughout the time course and showed the lowest degree of intra-sample variation based on SD and CV% of C_p. The 16S rRNA gene of V_2 was not signi-ficantly different from 16S rRNA of LT_1 with *p* values of 0.072 demonstrating an accepted level of gene expres-sion variability. The findings also show the similar growth and diesel degradation patterns of both isolates as shown in Figure 1. Hence, the expressions of 16S rRNA of both isolates were used to normalize all other target gene expressions respectively for comparison.

The target gene expressions and comparison between LT_1 and V_2 isolates

The expression levels of *rub*A, *alk*M, *alk*R, and *xcp*R genes in LT_1 samples exhibited their maximums during the initial stages of incubation (Figures 2 and 3a) and with high degrees of intra-sample variation in C_p with SD and CV% (Table 3). The higher expression (8.71×10^{12} gene copies) of *alk*M gene was observed at day 10 as compared to other genes involved and its expression declined as incubation time progressed. The above results revealed the involvement of these gene products of LT_1 in the diesel degradation. Previous studies showed that *Acinetobacter* sp. strain ADP1 requires at least five essential genes, namely *rub*A, *rub*B, *alk*M, *alk*R, and *xcp*R, for *n*-alkane utilisation (Ratajczak et al., 1998) confirming *rub*A, *rub*B, and *alk*M constitute a three component alkane hydroxyase system in *A. calcoaceticus* (Ratajczak et al., 1998; Geißdörfer et al., 1999; van Beilen et al., 2002). The overall *alk*R gene expression of LT_1, samples was comparatively low in relation to the alkane hydroxylase complex genes, *alk*M and *rub*A. This inference is in accordance with preceding studies that found *alk*R to be expressed at lower levels during alkane degradation despite its indispensability in the degradation process (Ratajczak et al., 1998). The *xcp*R gene encodes a type IV pilus-related system that may not only be required for the secretion of proteins but may represent a more universal transport system for a variety of macromolecules. It may also facilitate the alleviation of membrane stress incurred by bacterial cells during alkane degradation (Parche et al., 1997). All genes except *lip*B gene demonstrated a similar pattern. The *lipB* gene was expressed in LT_1 at all sampling times, however, low expression levels was observed as depicted by the high C_p values (Table 3). Unlike other target genes that were expressed in the early stage of diesel degradation, expression levels of *lipB* gene increased with incubation time (from 5.62×10^8 gene copies at day 10 to 2.82×10^9 gene copies at day 20) for LT_1 and

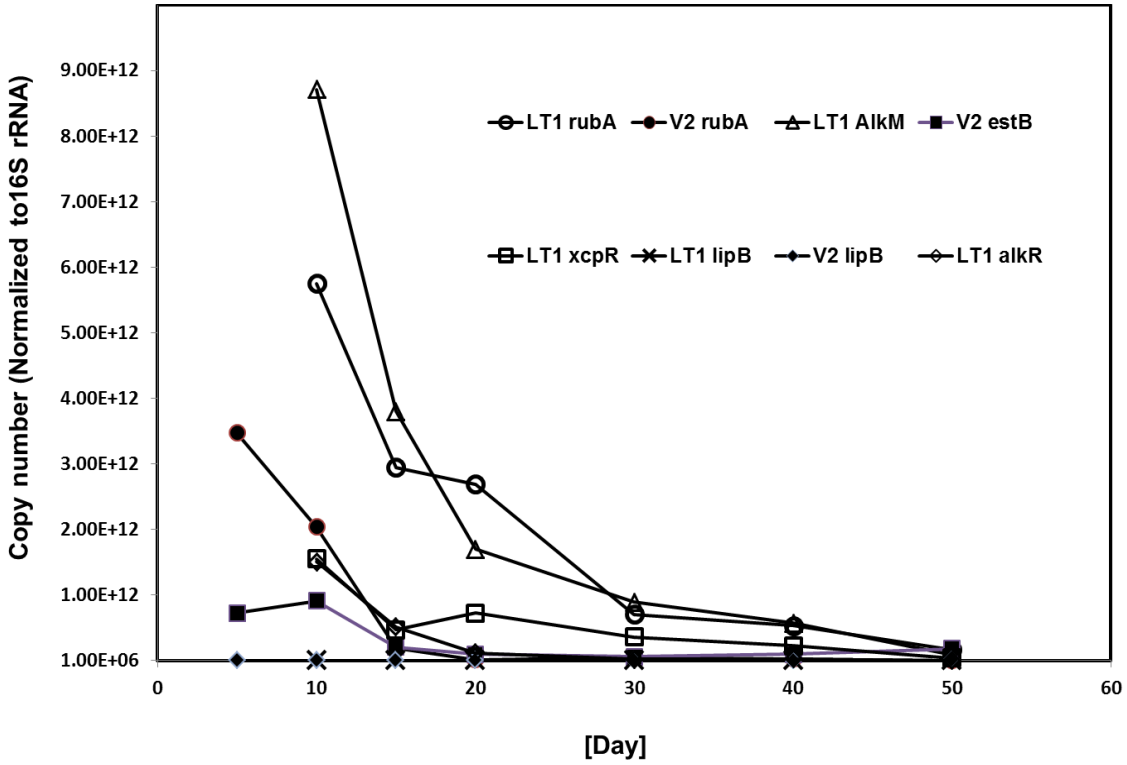

Figure 2. Expression profiles of *alk*M, *rub*A, *xcp*R, *lip*B and *alk*R genes of *A. calcoaceticus* LT_1 and of *rub*A, *est*B and*lip*B genes of *A. calcoaceticus* V_2.

declined thereafter showing greater intra-sample variation (SD and CV% values of 10.27 and 25.10 respectively) (Table 3). Positive peak formations of desired *est*B and *lip*A gene products were observed for many samples. However, such peaks are a consequence of amplification occurring very late in the PCR often with C_p values > 51.00 in a 55 cycle amplification segment, therefore are considered invalid and are indicative of false-positive results. Lack of target-specific amplifications of *est*B and *lip*A in LT_1 samples, suggest either the absence of gene expressions or low levels of expression.

In comparison with the diesel-degrading target gene expression levels of LT_1, the expression profile of the *rub*A gene of V_2 had a similar trend as LT_1 (Figure 2), exhibiting the maximum during the initial stage of incubation and declining as incubation time progressed. The *rub*A expression level of V_2 was down-regulated by the factor 10.115 as compared to that of LT_1. Despite the down-regulation, expression levels for *rub*A of V_2 were not significantly different from *rub*A of LT_1 with *p* values of 0.066.

During the amplification of *alk*M of V_2 samples, the *alk*M primer pair concurrently amplified the anticipated *alk*M gene (designated as *alk*M1 as shown in Figure 3A with a T_m of 80.36°C) as well an additional product; presumed to be another alkane hydroxlase that was tentatively designated *alk*M2 exhibiting a much higher T_m exceeding 92°C (Figure 3B) that was evident between 20 and 50 days of incubation. Amplification of *alk*M_1 and *alk*M_2 genes of V_2 samples was repeated and results were highly reproducible. Agarose gel electrophoresis of *alk*M_1 amplicons from LT1 confirmed the presence of the anticipated product of 189 bp from day 5 to 60 (Figure 3Ca). An additional product of 336 bp was evident (Figure 3Cb) from day 20 to 50 of V_2 samples which coincided with the melting curve analysis of *alk*M gene. The *alk*M gene amplified products of the V_2 at day 15 and LT_1 were sequenced and aligned. Partial sequence alignment (Figure 3D) shows 100% homogeneity of these two sequences. The *alk*M gene of LT_1 samples is therefore analogous to *alk*M_1 of V_2 isolate. Additionally, the obtained sequences showed 99 and 95% homogeneities with the partial sequences of alkane monoxygenase (*alkB*) from *Acinetobacter* sp. 49A and *A. calcoaceticus* PHEA-2, respectively. Sequencing of the day 20 sample of *alk*M_2 gene from isolate V_2 proved to be unsuccessful even after numerous attempts.

Formation of additional products could also be attributed to co-amplification of two or more genes as a result of sequence similarity. The presence of multiple alkane hydroxylases in a single bacterial strain is not an atypical occurrence (Tani et al., 2001; Marín et al., 2003).

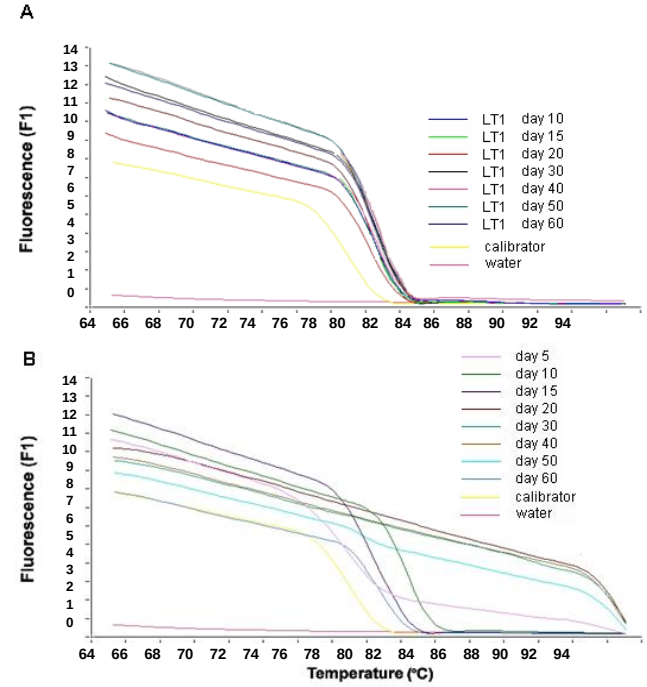

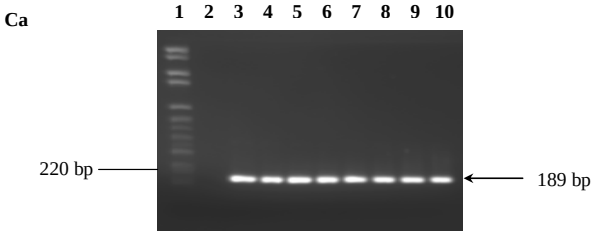

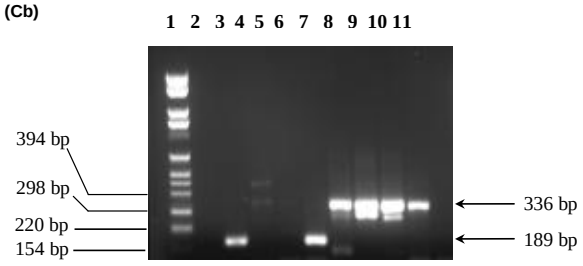

(D)

V_2-15 5'-ATTCACGTCTTGTGAAGAGTTTTATTCCACTGCAATATGCTGCAAATGTTTATGCATGTT

LT_1 5'-ATTCACGTCTTGTGAAGAGTTTTATTCCACTGCAATATGCTGCAAATGTTTATGCATGTT

49A *alkB5* 5'-ATTCACGTCTTGTGAAGAGTTTTATTCCACTGCAATATGCTGCAAATGTTTATGCATGTT

PHEA-2 5'-ATTCACGTCTTGTGAA**A**AGTTTTATTCCA**T**TGCAATATGCTGCAAATGTTTATGCATGTT

V_2-15 5'-ATTTAACAAGCCGTAAAACCACGTCATTCATTGATAAAATTTTGCTCGGTGTTTCGATG(

LT_1 5'-ATTTAACAAGCCGTAAAACCACGTCATTCATTGATAAAATTTTGCTCGGTGTTTCGATG(

49A *alkB5* 5'-ATTTAACAAGCCGTAAAACCACGTCATTCATTGATAAAATTTTGCTCGGTGTTTC**A**ATGG

PHEA-2 5'-ATTTAACAAGCCGTAAAAC**T**ACGTCATTCATTGATAAAATTTTGCTCGGTGTTTCAATGG

Figure 3. Melting curve analysis of *alk*M gene of (A) LT_1 and (B) V_2 samples, (Ca) Electrophoresed (2%) *alk*M1 gene amplicons of LT_1A. Lanes 1, Molecular weight marker IV (Roche); 2, negative control (no cDNA); 3, positive control; 4 - 10, day 5 to 60, respectively. (Cb) Electrophoresed *alk*M1 and *alk*M2 gene amplicons of V_2 samples --Lanes 1, Molecular weight marker IV (Roche); 2, negative control (no cDNA); 3, positive control; 4 - 11, days 5 to 60, respectively. (D) Partial sequence alignment of *alk*M1 amplicons of LT_1, V_2 and partial sequences of alkane monooxygenase of *A. calcoaceticus* PHEA-2; *Acinetobacter* sp. 49A.

Table 3. Descriptive statistics and variation data output for target genes of LT_1, and V_2 samples.

Factor	16S rRNA	*rub*A	*alk*M	*alk*R	*lip*A	*lip*B	*xcp*R	*est*B
LT_1								
n	7	7	7	7	7	7	7	7
Sample means	12.27	25.46	32.14	39.48	-	40.94	34.58	-
Min	10.32	23.02	29.7	35.46	-	37.08	31.98	-
Max	13.56	28.55	35.57	44.50	-	46.30	37.90	-
SD	1.27	3.55	4.06	10.11	-	10.27	3.63	-
CV (%)	10.31	13.92	12.65	25.60	-	25.10	10.49	-
V_2								
n	8	8	8	8	8	8	8	8
Sample means	12.29	29.09	*	*	-	39.76	*	31.81
Min	9.542	23.84	*	*	-	37.70	*	29.34
Max	16.86	34.50	*	*	-	41.23	*	33.58
SD	6.61	10.48	*	*	-	1.41	*	2.38
CV (%)	53.81	36.02	*	*	-	3.55	*	7.47

- Invalid C_p values due to nonspecific binding; * invalid C_p values due to multiple product formation. Analysis of 16S rRNA gene expression.

Multiple alkane hydroxylases enable alkane degraders to grow on a broad range of alkane substrates, where each alkane hydroxylase may exhibit unique properties and have different induction patterns (van Beilen et al., 2003). The *alk*Ma and *alk*Mb expressions of *Acinetobacter* sp. M1 were differentially induced in response to *n*-alkane chain length (van Beilenet al., 2003). Differential expressions of *alk*B1 and *alk*B2 of *P. aeruginosa* were not based on alkane chain length but rather on the levels of oxygen (Marín et al., 2003). In addition to two genes encoding AlkB-type alkane hydroxylase homologues in *Acinetobacter* sp. strain DSM 17874, *almA*, which encodes a putative flavin-binding monooxygenase, was also involved in the metabolism of long-chain n-alkanes (Throne-Holst et al., 2007). The *A. venetianus* VE-C3 genome possesses different alkane degrading genes which encode AlkB-like, soluble cytochrome P450 monooxygenases, AlmA and LadA (Fondi et al., 2013). V_2 might have been evolved to possess at least two alkane hydroxlases/monooxygenases to cope with the stress of the longer carbon chain length and/or under oxygen levels as *alk*M1 was expressed at the late exponential/early stationary phase and *alk*M2 throughout the late stationary phase.

In compliance with multiple *alk*M gene expressions, multiple *alk*R and *xcpR* genes of V_2 samples were also expressed to enhance the regulation of *alk*M expression (Figure 4). The expected amplification product of *alk*R gene in LT_1 samples, was only observed at late stage of degradation (days 30, 50, and 60) and in the V_2 samples, and there was shift in T_m of approximately 2°C for day-30 and 60 samples (Figure 4A). The presence of a second product (*alk*R2) with T_m exceeding 84°C was also observed at the early stage of diesel degradation (days 5, 10 and 15 samples). Despite the disparity in T_m, the amplification product size was identical to that of day 50. No *alk*R amplification occurred for days 20 and 40 samples. The *alk*R_1 gene of V_2 might be analogous to *alk*R of LT_1 on the basis of T_m and amplification product size. *A. calcoaceticus* sp. M1 that contained the two alkane hydroxylases *alk*Ma and *alk*Mb was also found to possess two transcription regulators *alk*Ra and *alk*Rb (Tani et al., 2001). Each alkane hydroxylase was regulated by either *alk*Ra or *alk*Rb responded to the alkane chain lengths. The *alk*R_1 gene of V_2 is comparable to *alk*R of LT_1 on the basis of T_m and amplification product size.

The *xcpR* gene, that encodes a subunit of the general secretory pathway, is required for alkane degradation in *Acinetobacter* sp. ADP1 and DSM 17874 strains (Parche et al., 1997; Throne-Holst et al., 2007). The expression of *xcp*R in conjunction with *rub*A and *rub*B in *A. calcoaceticus* is known to be constitutive (Ratajczak et al., 1998). Figure 4B shows that the presence of additional amplification products for *xcp*R of V_2 samples, illustrated by three defined peaks, exhibited higher T_ms. The results obtained for V_2 samples were highly reproducible yielding multiple products with identical melting temperatures. Real-time PCR amplification products of *xcp*R of V_2 samples were verified by gel electrophoresis (Figure 5). The presence of two distinct products was observed. The expected 192 bp product (*xcp*R1) was observed in all samples and the presence of a larger fragment of approximately 500 bp (*xcp*R2) was also observed in all samples except on days 30 and 40. The metabolism of *n*-alkanes in the V_2 isolate appears to be more complex. Its

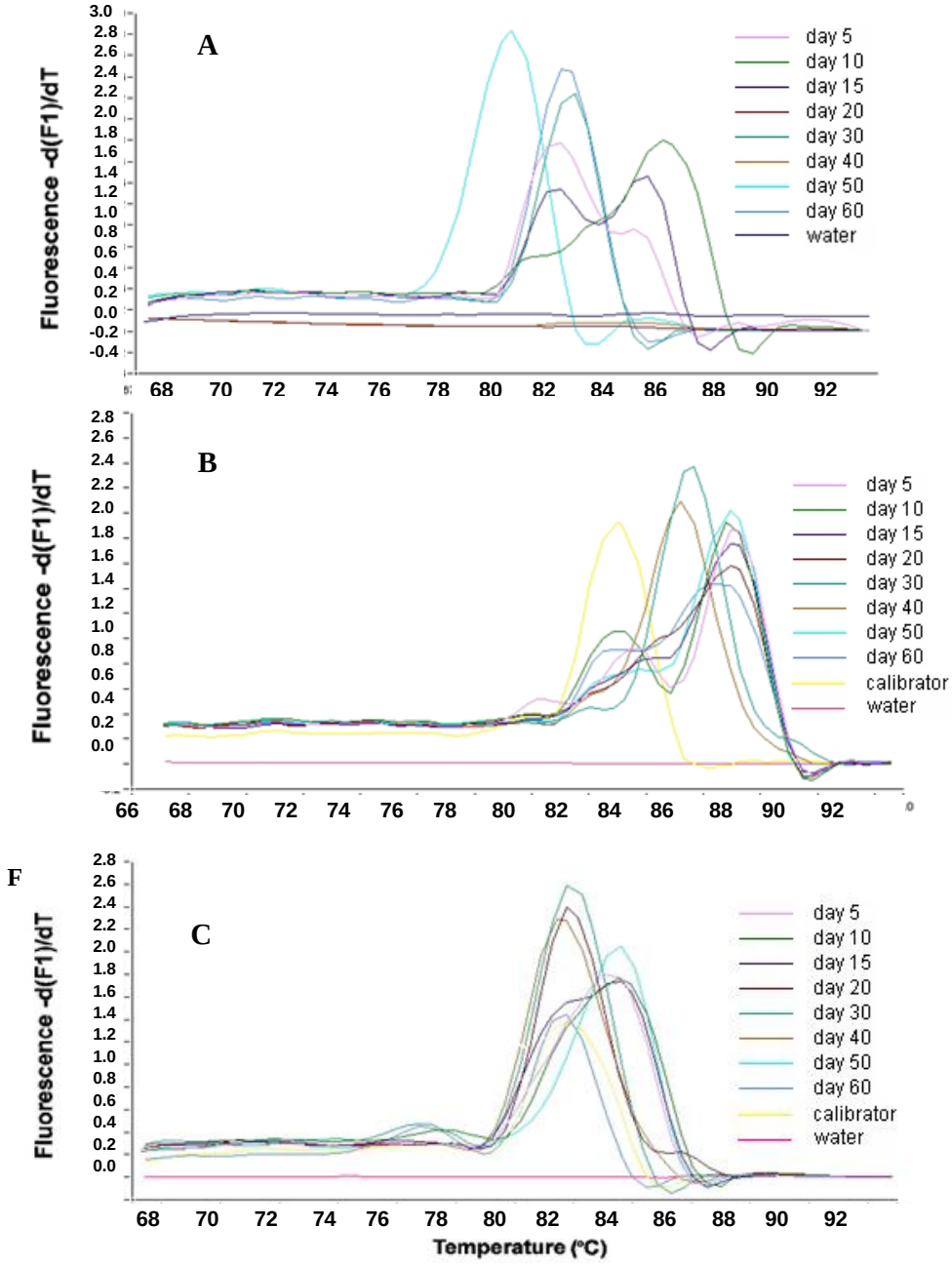

Figure 4. Melting peak analysis of (A)*alk*R gene,(B) *xcp*R and (C) *lip*B gene of V_2 samples determined by plotting the negative derivative of fluorescence [-d(F1)/dT].

broad substrate range, diversity and functions of the enzymes involved in alkane degradation, and its contrasting regulation of both constitutive and differential gene expression may be reminiscent of the fact that two and perhaps more *xcp*R genes are required to provide an adequate transport system during alkane degradation.

Rubredoxin (*rub*A) activity was detected in all investigated samples of LT_1 and V_2 isolates. LT_1 and V_2 samples exhibited similar *rub*A expression trends and the differences in expression levels were not significant. However, rubredoxinreductase (*rubB*) activity was not detected in any of the isolates despite rigorous optimising strategies and redesigning of primers. Plausible reasons for the inability to detect *rub*B activity could be attributed to very low expression levels, or poor primer design.

Theoretically, *rub*B would have exhibited a similar

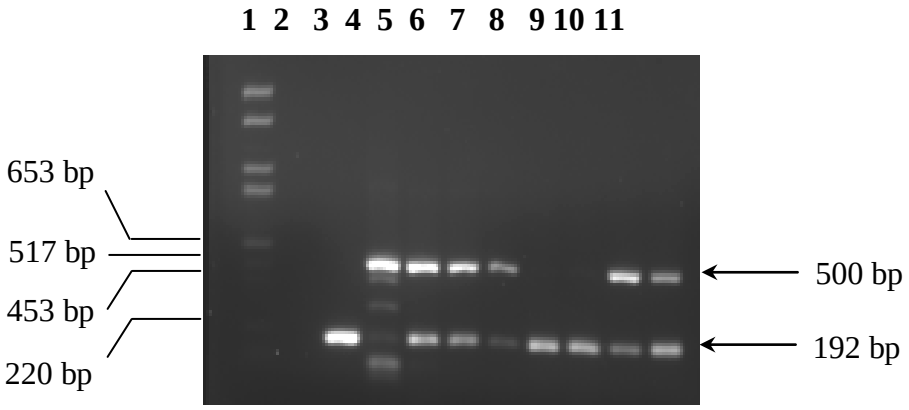

Figure 5. Electrophoresed *xcp*R amplicons of V_2 samples. Lanes 1- molecular weight marker VI (Roche); 2- negative control (no cDNA template); 3- positive control (calibrator); 4 to 11- *xcp*R amplicons of 5 to 60 days samples, respectively.

expression trend to that of *rub*A due to their synergistic association (Geißdörfer et al., 1999). Interestingly, novel genes encoding AlkB-Rubredoxin fusion proteins were used in the hydroxylation of long-chain alkanes by Gram positive bacteria (Nie et al., 2011). In addition, rubredoxin-rubredoxin reductase systems are present in many other organisms that are unable to degrade alkanes, where they serve other functions such as rapid transport of reducing equivalents to the final receptor (Hagelueken et al., 2007).

Although, *rub*A, *rub*B and *est*B constitute an operon in *Acinetobacter* sp. ADP1, it was established that no association could be ascertained between the expression of *rub*A and *est*B in accordance with the findings by Geißdörfer et al. (1999). The expression of *est*B was predominantly observed in V_2 samples and either non-expression or extremely low expression of the *est*B gene in LT_1 samples (Figure 3). During the diesel degradation phase of V_2 inocula, an opaque, waxy material was observed, probably due to bioemulsifiers in the hydrocarbon and hydrocarbon-culture medium fraction, but not in flasks containing LT_1 inocula. These findings are suggestive that the involvement of *est*B in the release of the bioemulsifier may be plausible (Shabtai and Gutnick, 1985).

Low expression of *lip*A in LT_1 and lack of expression in V_2 (Table 3) is an indication of its non-involvement in the degradation of diesel. The *lipB* gene was expressed in all samples in this study. Expression of *lip*B amongst V_2 samples was moderately constant exhibiting lower SD and CV% values of 1.41 and 3.55, respectively (Table 3). The expression profile of *lip*B gene in V_2 (Figure 4C) was found in low level, depicted by the high C_p values exhibiting maximum expression at day 15. Thereafter, expression levels declined fairly constantly. In comparison to LT_1, *lip*B of V_2 was up-regulated by the factor 1.976 with no significant difference (p= 0.436). In this study, the expression trends of *lipA* and *lipB* were incongruent, and expression of *lipB* was still evident in the absence of *lipA* expression amongst V2 samples. The *lipB* gene encodes a lipase chaperone that prevents the complete folding of the lipase before it traverses the outer cell membrane (Kim et al., 2008). Alternatively, steric chaperones may have other functions such as the autotransporter protein that can be used to direct a variety of proteins to the cell surface in addition to LipA folding (Wilhelm et al., 2007). Kim et al. (2008) also reported that there are 3 different *lipa*A genes present in *Acinetobacter* sp. DYL 129. The involvement of *lip*A *and lip*B in alkane degradation is still unknown.

The findings of this study confirm the importance of *rubA, alkM, alkR,* and *xcpR* genes in the process of alkane degradation. The results are also suggestive that different members of the alkane degraders, such as *Acinetobacter* LT_1 and V_2 strains in this study employ a variety of alkane degrading pathways for alkane oxidation, albeit both isolates achieved comparable levels of diesel degradation. It is apparent that alkane oxidation in V_2 appears to be complex due to its diverse regulations of multiple alkane hydroxylases, alkane hydroxylase transcription regulators and the secretory pathways. However, involvement of other alkane degrading proteins such as cytochrome P450 alkane hydroxylases, Lad and AlmA cannot be ruled out.

Conclusions

We concluded that both *Acinetobacter* strains LT_1 and V_2 in this study showed comparable diesel degrading ability, however real-time PCR experiments revealed more than one enzyme system involved by V_2 indicating its diverse regulations of multiple alkane hydroxylases, its transcription regulators and the secretory pathways. Low or no expression of *lipB* and *lip*A genes suggested the absence

of lipases in degradation. This study also confirms the importance of *rubA, alkM, alkR* and *xcpR* genes in the process of alkane degradation, although, future experiments would be necessary to elucidate the involvement of other proteins such as cytochrome P450 alkane hydroxylases, Lad and AlmA in alkane degradation.

ACKNOWLEDGEMENTS

This research was funded by the National Research Foundation of South Africa. The authors are grateful to the NRF for the award of doctoral bursary.

REFERENCES

Coon MJ (2005). Omega oxygenases: nonheme-iron enzymes and P450 cytochromes. Biochem. Biophys. Res. Commun. 338: 378–385.

Fondi M, Orlandini V, Emiliani G, Papaleo MC, Maida I, Perrin E, Vaneechoutte M, Dijkshoorn L, Fani R (2012). Draft genome sequence of the hydrocarbon-degrading and emulsan-producing strain *Acinetobacter venetianus* RAG-1T. J. Bacteriol. 194(17): 4771-4772. Doi: 10.1128/JB.01019-12.

Fondi M, Rizzi E, Emiliani G, Orlandini V, Berna L, Papaleo MC, Perrin E, Maida I, Corti G, De Bellis G, Baldi F, Dijkshoorn L, Vaneechoutte M, Fani R (2013). The genome sequence of the hydrocarbon-degrading *Acinetobacter venetianus* VE-C3. Res. Microbiol. 164(5): 439-449.

Geißdörfer W, Kok RG, Ratajczak A, Hellingwerf KJ, Hillen W (1999) The genes *rubA*and *rubB*for alkane degradation in *Acinetobacter*sp. strain ADP1 are in an operon with *estB*, encoding an esterase, and *oxyR*. J. Bacteriol.181(14): 4292-4298.

Hagelueken G, Wiehlmann L, Adams TM, Kolmar H, Heinz DW, Tümmler B, Schubert W-D (2007). Crystal structure of the electron transfer complex rubredoxin–rubredoxinreductase of *Pseudomonas aeruginosa*. PNAS 104(30): 12276-12281.

Jung J, Baek JH, Park W (2010). Complete genome sequence of the diesel-degrading *Acinetobacter* sp. strain DR1. J. Bacteriol. 192(18): 4794-4795.

Kang YS, Jung J, Jeon CO, Park W (2011). *Acinetobacteroleivorans* sp. nov. is capable of adhering to and growing on dieseleoil. J. Microbiol. 49: 29-34.

Kim S-H, Park I-H, Lee S-C, Lee Y-S, Zhou Y, Kim C-M, Ahn S-C, Choi Y-L (2008). Discovery of three novel lipase (*lipA$_1$, lipA$_2$,* and *lipA$_3$*) and lipase-specific chaperone (*lipB*) genes present in *Acinetobacter* sp. DYL129. Appl. Genet. Mol. Biotechnol. 77(5): 1041-1051.

Kotani T, Kawashima Y, Yurimoto H, Kato N, Sakai Y (2006). Gene structure and regulation of alkane monooxygenases in propane-utilizing *Mycobacterium* sp. TY-6 and *Pseudonocardia* sp. TY-7. J. Biosci. Bioeng. 102: 184–192.

Kotani T, Yurimoto H, Kato N, Sakai Y (2007). Novel acetone metabolism in a propane-utilizing bacterium, *Gordonia* sp. strain TY-5. J. Bacteriol. 189: 886–893.

Kubista M, Andrade JM, Bengtsson M, Forootan A, Jonák J, Lind K, Sindelka R, Sjöback R, Sjögreen B, Strömbom L, Ståhlberg A, ZoricN (2006) The real-time polymerase chain reaction. Mol. Aspects Med. 27: 95-125.

Lee M, Woo S-G, Ten LN (2012). Characterization of novel diesel-degrading strains *Acinetobacterhaemolyticus* MJ01 and *Acinetobacter johnsonii* MJ4 isolated from oil-contaminated soil. World J. Microbiol. Biotechnol. 28: 2057–2067.

Mandri T, Lin J (2007). Isolation and characterization of engine oil degrading indigenous microorganisms in KwaZulu-Natal, South Africa. Afr. J. Biotechnol. 6(1): 23-27.

Mara K, Decorosi F, Viti C, Giovannetti L, Papaleo MC, Maida I, Perrin E, Fondi M, Vaneechoutte M, Nemec A, van den Barselaar M, Dijkshoorn L, Fani R (2012) Molecular and phenotypic characterization of *Acinetobacter* strains able to degrade diesel fuel. Res. Microbiol. 163: 161-172.

Marchesi JR, Sato T, Weightman AJ, Martin TA, Fry JC, Hiom SH, Wade WG (1998). Design and evaluation of useful bacterium-specific PCR primers that amplify genes coding for bacterial 16S rRNA. Appl. Environ. Microbiol. 64: 795-799.

Marín M, Yuste L, RojoF (2003) Differential expression of the components of the two alkane hydroxylases from *Pseudomonas aeruginosa.* J. Bacteriol. 185(10): 3232-3237.

Marquez-Rocha FJ, Hernandez-Rodriguez V, Lamela MT (2001). Biodegradation of diesel oil in soil by a microbial consortium. Water Air Soil Pollut. 128: 313-320.

Nie Y, Liang J, Fang H, Tang Y-Q, Wu X-L (2011). Two novel alkane hydroxylase-rubredoxin fusion genes isolated from a Dietzia bacterium and the functions of fused rubredoxin domains in long-chain n-alkane degradation. Appl. Environ. Microbiol. 77(20): 7279–7288.

Parche S, Geißdörfer W, Hillen W (1997) Identification and characterization of *xcpR*encoding a subunit of the general secretory pathway necessary for dodecane degradation in *Acinetobacter calcoaceticus* ADP1. J. Bacteriol. 179(14): 4631-4634.

Pfaffl MW, Horgan GW, Dempfle L (2002). Relative Expression Software Tool (REST-XL ©) for group-wise comparison and statistical analysis of relative expression results in real-time PCR. Nucleic Acids Res. 30(9): e36

Rasmussen RP (2001). Quantification on the LightCycler. In: Meuer S, Wittwer C, Nakagawara K (eds). RapidCycle Real-time PCR, Methods and Applications. Springer Press, Heidelberg. pp. 21-34.

Ratajczak A, Geißdörfer W, HillenW (1998) Expression of alkane hydroxylase from A*cinetobacter*sp. strain ADP1 is induced by a broad range of *n*-alkanes and requires the transcriptional activator AlkR. J. Bacteriol.180(22): 5822-5827.

Rojo F (2009). Degradation of alkanes by bacteria. Environ. Microbiol. 11: 2477-2490.

Rojo F (2010). Enzymes for aerobic degradation of alkanes. In: Timmis KN (ed) Handbook of hydrocarbon and lipid microbiology. Springer, Germany, Vol 2, pp. 781–797.

Shabtai Y, GutnickDL (1985). Exocellular esterase and emulsan release from the cell surface of *Acinetobactercalcoaceticus*. J. Bacteriol. 161(3):1176-1181.

Singh C, Lin J (2008) Isolation and characterization of diesel oil degrading indigenous microorganisms in Kwazulu-Natal, South Africa. Afr. J. Biotechnol. 7(2): 1927-1932.

Tani A, Ishige T, Sakai Y, Kato N (2001). Gene structures and regulation of the alkane hydroxylase complex in *Acinetobacter* sp. strain M-1. J. Bacteriol. 183: 1819-1823.

Tani A, Ishige T, Sakai Y, KatoN (2002). Two acyl-CoA dehydrogenases of *Acinetobacter* sp. strain M- 1 that uses very long-chain *n*-alkanes. J. Biosci. Bioeng. 94(4): 326-329.

Throne-Holst M, Wentzel A, Ellingsen TE, Kotlar H-K, Zotchev SB (2007). Identification of novel genes involved in long-chain n-alkane degradation by *Acinetobacter* sp. Strain DSM 17874. Appl. Environ. Microbiol. 73(10): 3327–3332.

van Beilen JB, Funhoff EG (2007). Alkane hydroxylases involved in microbial alkane degradation. Appl. Microbiol. Biotechnol. 74: 13-21.

van Beilen JB, Li Z, Duetz WA, Smits THM, Witholt B (2003). Diversity of alkane hydroxylase systems in the environment. Oil Gas Sci. Technol. 58: 427-440.

van Beilen JB, Neuwenschwander M, Smits THM, Roth C, Balada SB, Witholt B (2002). Rubredoxins involved in alkane oxidation. J. Bacteriol. 184: 1722-1732.

van Hamme JD, Singh A, Ward OP (2003). Recent advances in petroleum microbiology. Microbiol. Mol. Biol. Rev. 60(4): 503-549.

Watkinson RJ, Morgan P (1990). Physiology of aliphatic hydrocarbon-degrading microorganisms. Biodegradation 1(2-3): 79-92.

Wentzel A, Ellingsen TE, Kotlar HK, Zotchev SB, Throne-Holst M (2007). Bacterial metabolism of long-chain n-alkanes. Appl. Microbiol. Biotechnol. 76: 1209–1221.

Wilhelm S, Rosenau F, Becker S, Buest S, Hausmann S, Kolmar H, Jaeger K-E (2007). Functional Cell-Surface Display of a Lipase-Specific Chaperone. Chem. BioChem. 8(1): 55-60.